Beam Optimization for Digital Mammography – II

Mark B. Williams[1], Priya Raghunathan[1], Anthony Seibert[2], Alex Kwan[2], Joseph Lo[3], Ehsan Samei[3], Laurie Fajardo[4], Andrew D.A. Maidment[5], Martin Yaffe[6], and Aili Bloomquist[6]

[1] University of Virginia
[2] University of California-Davis
[3] Duke University
[4] University of Iowa
[5] University of Pennsylvania
[6] University of Toronto

Abstract. Optimization of acquisition technique factors (target, filter, and kVp) in digital mammography is required for maximization of the image SNR, while minimizing patient dose. The goal of this study is to compare, for each of the major commercially available FFDM systems, the effect of various technique factors on image SNR and radiation dose for a range of breast thickness and tissue types. This phantom study follows the approach of an earlier investigation [1], and includes measurements on recent versions of two of the FFDM systems discussed in that paper, as well as on three FFDM systems not available at that time. The five commercial FFDM systems tested are located at five different university test sites and include all FFDM systems that are currently FDA approved. Performance was assessed using 9 different phantom types (three compressed thicknesses, and three tissue composition types) using all available x-ray target and filter combinations. The figure of merit (FOM) used to compare technique factors is the ratio of the square of the image SNR to the mean glandular dose (MGD). This FOM has been used previously by others in mammographic beam optimization studies [2],[3]. For selected examples, data are presented describing the change in SNR, MGD, and FOM with changing kVp, as well as with changing target and/or filter type. For all nine breast types the target/filter/kVp combination resulting in the highest FOM value is presented. Our results suggest that in general, technique combinations resulting in higher energy beams resulted in higher FOM values, for nearly all breast types.

1 Introduction

The criteria for optimization of tube voltage and external filtration in full field digital mammography (FFDM) differ from those used in screen-film mammography. This is in part because the separation of the processes of acquisition and display in the former permits the contrast of individual structures to be adjusted when the image is viewed. Thus, rather than maximization of contrast within the constraint of acceptable film darkening and patient dose, beam optimization in digital mammography requires maximization of the image SNR, constrained by acceptable patient dose [4]. In recent

Susan M. Astley et al. (Eds.): IWDM 2006, LNCS 4046, pp. 273 – 280, 2006.

years, four FFDM systems have gained FDA approval, with others soon to follow. Most of those systems are equipped with mechanisms for automatic selection of at least some technique factors including mAs and in some cases kVp, filtration, and target material. In some units, different acquisition modes are available in which different look-up-tables are utilized to emphasize either subject contrast (with lower kVp and higher mAs) or low dose (with higher kVp and lower mAs). It is the goal of this study to examine, for three simulated breast compositions, and three simulated breast thicknesses, the effect on the image SNR and the mean glandular dose (MGD) of varying kVp, and target and filter type.

2 Methods

Five different FFDM systems, the GE Healthcare Senographe 2000D, the Siemens Mammomat Novation, the Lorad Selenia, the Fischer/Hologic Senoscan, and Fuji's mammographic storage phosphor system, were used to image a common set of phantoms made of blocks of breast equivalent material (CIRS, Inc., Norfolk, VA). Nine different phantoms were assembled and imaged, simulating breasts of three different thicknesses (3 cm, 5 cm, and 7 cm), and three different attenuation equivalent adipose/fibroglandular mass ratios (30/70, 50/50, and 70/30). Two 5 mm thick blocks were placed on the top and bottom of each stack, to simulate skin (Fig. 1). The skin blocks were 100% adipose equivalent material.

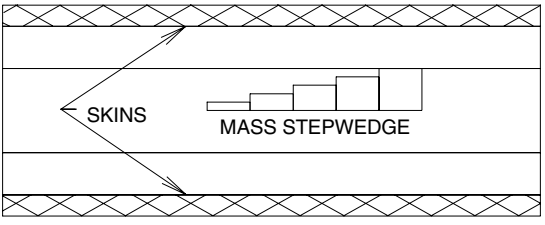

Fig. 1. Side view of a 5 cm phantom with a 2 cm signal block at the center, two 1 cm blank blocks and two 0.5 cm skins on the surface

In each phantom stack assembled, the centrally located block in the stack (the signal block) contained two stepwedges, one each of calcification equivalent and mass equivalent material. The mass equivalent stepwedge has the same x-ray attenuation as 100% glandular equivalent material, and the microcalcification equivalent step wedge is composed of calcium carbonate (Fig. 2). The thickness of all signal blocks is 2 cm.

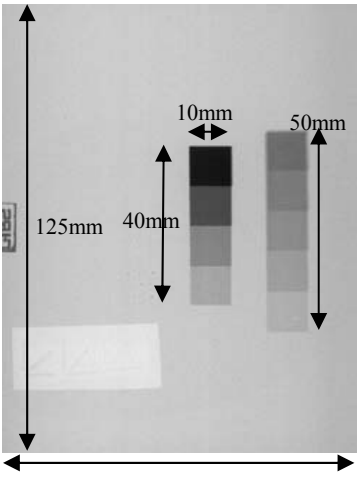

Fig. 2. Image of the phantom showing calcification (left) and mass equivalent step wedges.

Images were obtained in manual mode with the phantoms positioned at the chest wall edge of the receptor, centered left to right. Exposure time was selected to give approximately the same average pixel value in the phantom background area for each phantom/technique combination. For each combination, two images were obtained with identical exposure times for the purpose of image subtraction, taking care not to move the phantom between the two exposures. At each site, entrance exposures (mR/mAs) and half value layers (HVLs) were measured for each target/filter/kVp combination used. Table 1 lists the target and filter combinations and range of kVps used for each FFDM system tested in the study. Signal was defined as the difference between the average pixel values in a region of interest (ROI) centered on an individual step, and an equal sized ROI located immediately adjacent to the step, but containing only background.

Table 1. FFDM Units tested

System	Target	Filter	kV Range
Siemens	Mo, W	Mo,	23 – 35
Selenia	Mo	Mo,	23 – 39
Fischer	W	Al	28 – 37
GE	Mo, Rh	Mo,	24 – 32
Fuji	Mo	Rh	24 – 34

To quantify the image noise, the two images of a given phantom, obtained at a common technique, were subtracted. Image subtraction was performed to remove fixed pattern noise associated with phantom defects, detector nonuniformity, and heel effect. Noise in a single image was defined as the standard deviation of the pixel values in an ROI within the difference image, divided by the square root of two.

The MGD for each phantom was calculated using its known thickness, composition and the measured HVL and mR/mAs values from each FFDM system. For Mo/Mo and Mo/Rh spectra, the parameterized dose tables of Sobol and Wu were utilized to obtain the glandular dose per unit exposure [6]. For the W/Al spectra, normalized (to entrance exposure) MGD values were obtained from the data of Stanton et al. [7]. Their data were extrapolated to 3 cm breast thickness, and interpolation between their published HVL curves was used to obtain correction factors for the particular glandular volume fractions (0.22, 0.40, and 0.61, corresponding to glandular mass fractions of 0.30, 0.50, and 0.70, respectively) used in our study. For the W/Rh spectra, the calculations of Boone were utilized, interpolating between his published HVL and adipose/ fibroglandular composition values [5]. All FOM values were obtained by dividing the square of the SNR by the MGD expressed in units of 10^{-5} Gy (1 mRad).

3 Results

For a given phantom/target/filter combination, the form of the dependence of the signal on kVp was the same for all the steps of each stepwedge; only the magnitudes of the signals differed. Therefore, the results presented in this paper will use only the 0.3 mm thick microcalcification step for calculation of the signal. The plots of Figures 3 and 4 show examples of the dependence of SNR and dose per exposure, respectively, on changing kVp. In these examples, the FFDM systems are the Loard Selenia and Senography 2000D, respectively and the phantoms had 0.50 mass fraction. In Figure 3, the calculated SNR has been normalized by the average pixel value in the background region of the phantom image since the average pixel values were not exactly the same for all kVps tested.

The acquisition parameters chosen by the GE Senographe 2000D using its intrinsic Automatic Optimization of Parameters (AOP) system were recorded for every phantom thickness and composition combination. Automatically selected acquisition parameter values for other units equipped with such systems are currently in the process of being obtained.

Table 2 lists the target, filter and kVp that resulted in the maximum value of FOM for each breast type and system.

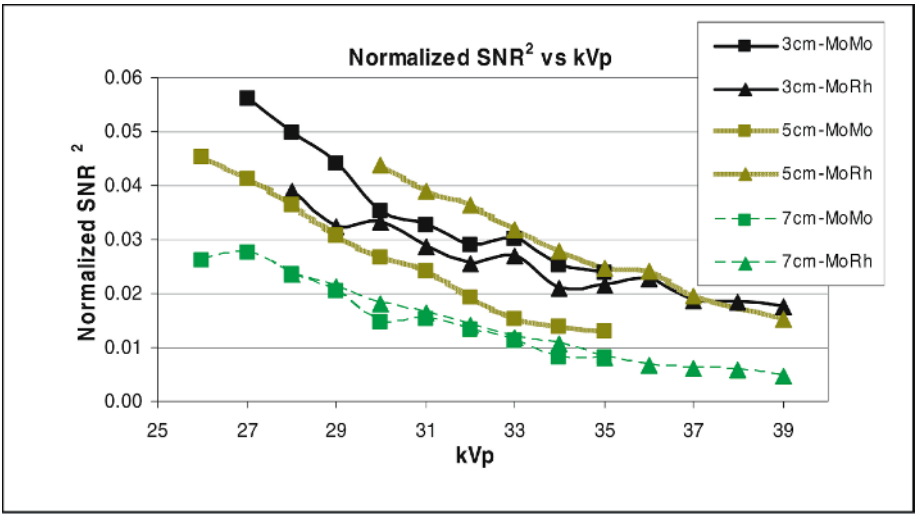

Fig. 3. Lorad Selenia : Square of SNR normalized by the average ADU value in the background, 50/50 composition

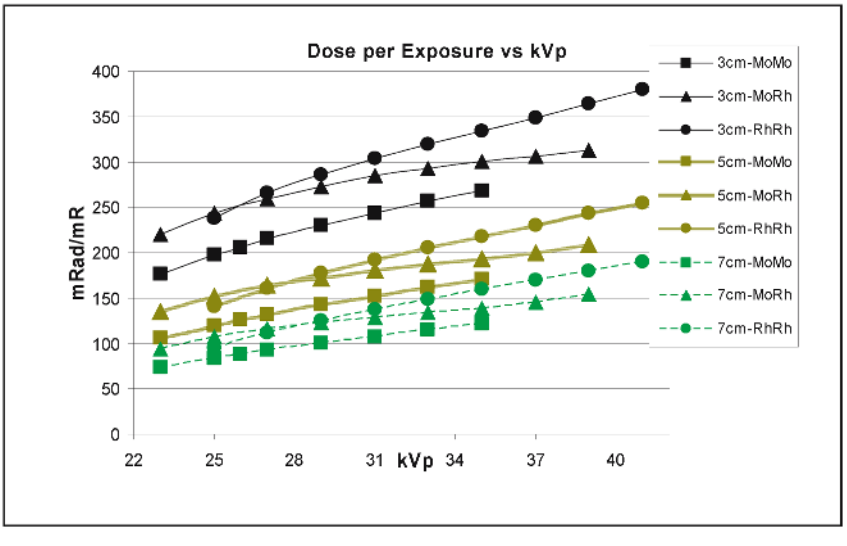

Fig. 4. GE : Dose per Exposure vs kVp, 50/50 composition

Table 2. Acquisition parameters resulting in maximum FOM. Table entries are in the form Target / Filter / kVp.

		30/70	50/50	70/30
GE	3cm	Mo / Mo / 25	Mo / Mo / 29	Mo / Mo / 29
	5cm	Rh / Rh / 27	Rh / Rh / 29	Rh / Rh/ 29
	7cm	Rh / Rh / 29	Rh / Rh / 29	Rh / Rh / 29
Lorad	3cm	Mo / Mo / 24	Mo / Rh / 28	Mo / Rh / 28
	5cm	Mo / Mo / 24	Mo / Mo / 25	Mo / Rh / 28
	7cm	Mo / Rh / 28	Mo / Rh / 28	Mo / Rh / 28
Siemens	3cm	W / Rh / 26	W / Rh / 29	W / Rh / 26
	5cm	W / Rh / 26	W / Rh / 26	W / Rh / 29
	7cm	W / Rh / 29	W / Rh / 29	W / Rh /29
Fuji	3cm	Mo / Mo / 24	Mo / Mo / 24	Mo / Rh / 30
	5cm	Mo / Mo / 24	Mo / Mo / 24	Mo / Rh / 30
	7cm	Mo / Rh / 30	Mo / Rh / 30	Mo / Rh / 31
Fischer	3cm	W / Al / 27	W / Al / 27	W / Al / 27
	5cm	W / Al / 29	W / Al / 30	W / Al / 30
	7cm	W / Al / 41	W / Al / 41	W / Al / 42

4 Discussion and Conclusions

The shape of the FOM vs. kVp curves for a given target/filter/phantom combination was found to be independent of step thickness, and was similar for mass and calcification equivalent signals. Figures 5-9 suggest that, for 5 cm breast thickness, for 50/50 as well as 70/30 compositions, the hardest beams result in higher FOM values in all systems tested. Furthermore, for 5 cm breast thickness and molybdenum target

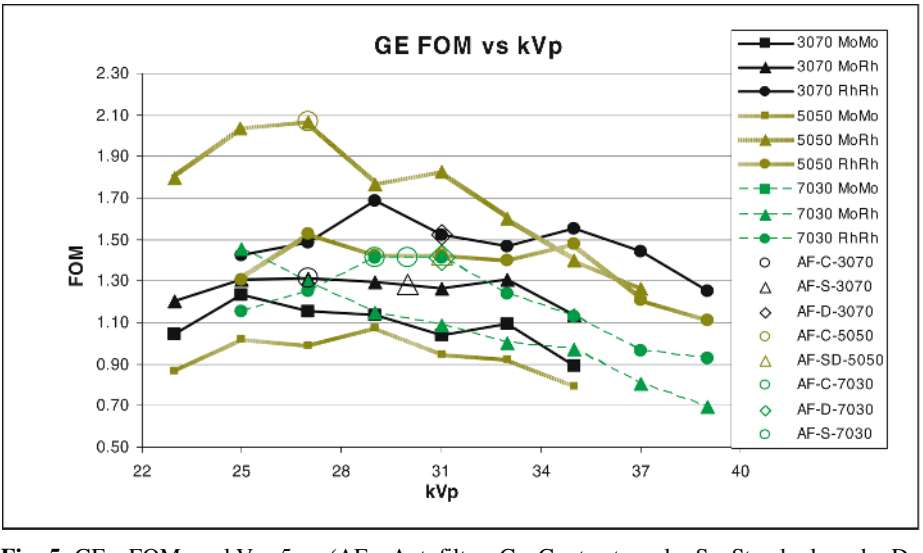

Fig. 5. GE : FOM vs. kVp, 5cm (AF : Autofilter, C : Contrast mode, S : Standard mode, D : Dose mode)

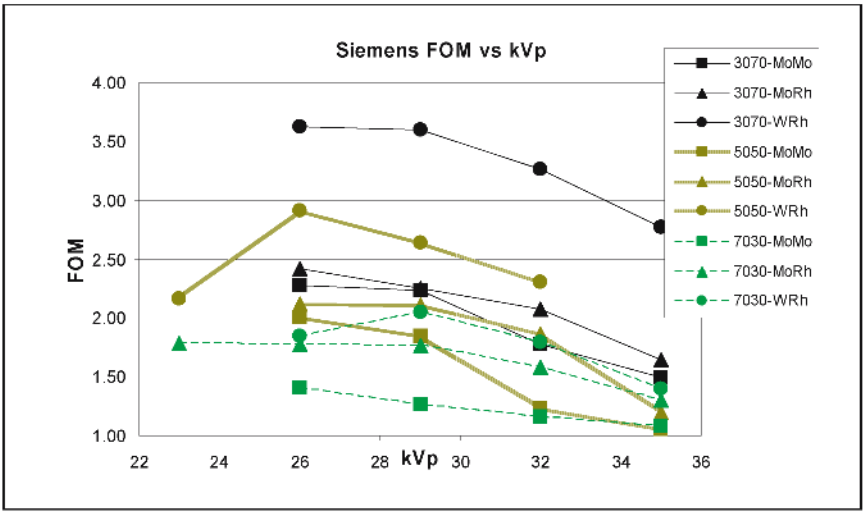

Fig. 6. Siemens : FOM vs. kVp, 5 cm

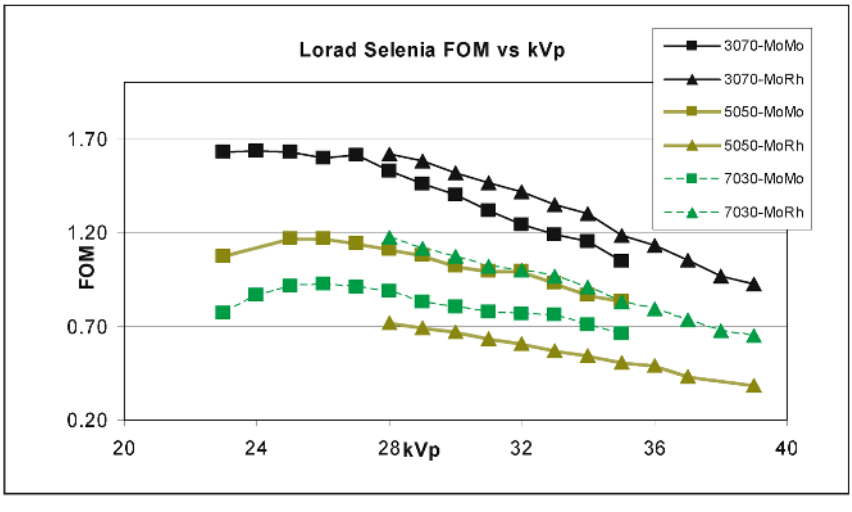

Fig. 7. Lorad Selenia : FOM vs. kVp, 5 cm

material, higher FOM values were obtained with rhodium filtration relative to molybdenum filtration for all breast compositions considered. Also, for 5 cm thick breasts, compared to molybdenum, tungsten targets resulted in higher FOM values for all compositions in the Novation. Space limitations prevent us from presenting data for 3 cm and 7 cm compressed breast thickness here. However, for the Senographe 2000D, the rhodium target resulted in higher FOM for all 5 cm and 7cm breasts. On the other hand, in nearly all cases the FOM is a relatively weak function of changing kVp, with few well-defined maxima.

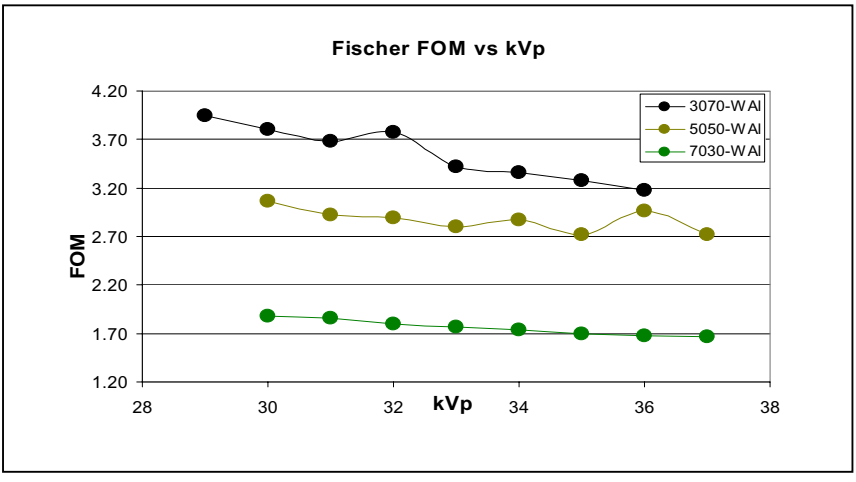

Fig. 8. Fischer : FOM vs. kVp, 5 cm

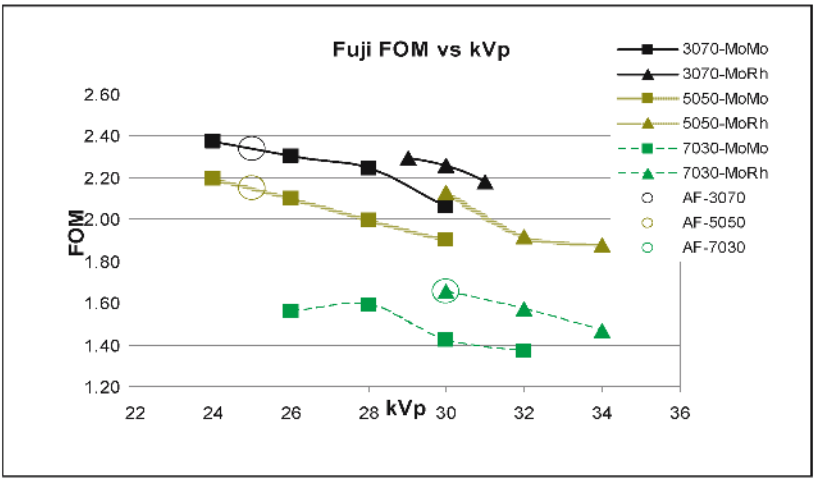

Fig. 9. Fuji : FOM vs. kVp, 5 cm (AF : AutoFilter)

These data suggest that the choice of target material and external filtration is more significant in determination of the overall FOM of a DM system than is choice of tube voltage. Figures 5 and 9 show the target/filter/kVp combination chosen by the Automatic Optimization of Parameters (AOP) and Autofilter systems of the GE Senographe 2000D and the mammography units used in testing the Fuji storage phosphor system. The selected techniques are indicated by the single, open symbols. As the figure shows, the technique factors selected by the AOP system are in most cases quite close to those that produced the highest FOM values in our study. A complete description of automated parameter selection performance across all manufacturers will be presented at the meeting.

Acknowledgements

We would like to thank the following people who helped obtain the significant amount of data needed for this study : Sandra Maxwell and Allen McGruder from the University of Iowa., Gordon Mawdsley and Sam Shen from the University of Toronto.

References

1. Williams MB, More MJ, Venkatakrishnan V, Niklason L, Yaffe MJ, Mawdsley G, Bloomquist A, Maidment ADA, Chakraborty D, Kimme-Smith C, and Fajardo LL. "Beam optimization for digital mammography". IWDM 2000: 5th International Workshop on Digital Mammography. (Martin J. Yaffe, Editor). Medical Physics Publishing. Madison, Wisconsin, 2001; 108-119
2. Boone, J., Shaber, G., and Tecotzky, M. (1990). Dual energy mammography: A detector analysis. Med.Phys. *17*, 665-675
3. Jennings, R.L., Quinn, P.W., Gagne, R.M., and Fewell, T.R. (1993). Evaluation of x-ray sources for mammography. Proc SPIE *1896*, 259-268
4. W., Sajewicz, A. M., Ogden, K. M. and Dance, D. R. Experimental investigation of the dose and image quality characteristics of a digital mammography imaging system. Med. Phys. **30**(3), 442–448 (2003)
5. Boone, J. (1999). Glandular breast dose for monoenergetic and high-energy x-ray beams: Monte Carlo assessment. Radiology 213, 23-37
6. Sobol, WT and Wu, X. Parameterization of mammography normalized average glandular dose tables. Medical Physics 24(4), 547-555. 1997
7. Stanton, L., Villafana, T., Day, J., and Lightfoot, D. (1984). Dosage evaluation in mammography. Radiology 150, 577-584